Monografías Matemáticas *García de Galdeano* **43**, 181–194 (2024)

OPTIMAL SHAPE AND LOCATION OF SENSORS FOR WAVE PRESSURE BOUNDARY MEASUREMENTS

Yannick Privat

Abstract. This conference paper is a synthesis of several works dedicated to the optimal positioning of sensors, when one wishes to reconstruct an acoustic pressure from measurements performed on the boundary of a domain. In a first step, we present a generic approach to address the issue of sensor shape and location optimization, based on the well-posedness of an inverse problem. In a second step, we try to show the limits of the previous approach, by presenting an example of application to a medical imaging problem, which is out of this framework and is therefore more difficult to deal with.

Keywords: wave equation, boundary observability, Rellich identity, shape optimization, tomography.

AMS classification: 49J20, 49K20, 35L05, 92C50.

§1. Introduction

We report on a series of works done in collaboration with M. Bergounioux, E. Bretin, E. Humbert, E. Trélat and E. Zuazua, concerning the problem of optimizing the shape and location of sensors for wave like systems.

Let $T > 0$ and Ω be a bounded connected open subset of $\mathbb{R}^n$ with Lipschitz boundary. The Lipschitz set $\partial\Omega$ is endowed with the $(n-1)$-dimensional Hausdorff measure $\mathcal{H}^{n-1}$. In the sequel, measurability of a subset $\Gamma \subset \partial\Omega$ is understood with respect to the measure $\mathcal{H}^{n-1}$. The purpose of this article is to introduce and analyze the issue of optimizing the shape and location of sensors for a hyperbolic source reconstruction problem for the homogeneous wave equation

$$\partial_{tt} y(t,x) - \Delta y(t,x) = 0 \quad (t,x) \in [0,T] \times \Omega. \tag{1}$$

Such a model arises in thermo-acoustic, photo-acoustic and ultrasound elastography models, in the confined domain Ω. The inverse problem at hand is: given a measurement (made by sensors) over a certain duration T of a pressure related quantity on $\partial\Omega$, or on a part of $\partial\Omega$, recover the initial pressure $y(0,x)$.

Of course, this problem is more relevant when $n = 3$, but as long as it is not specified otherwise, it is looked at here for any non-zero integer n.

Let us assume that on the boundary, the pressure is absorbed, which leads to consider homogeneous Dirichlet boundary conditions, in other words

$$y(t,x) = 0, \qquad (t,x) \in [0,T] \times \partial\Omega. \tag{2}$$

What is measured is the outgoing flux $\partial_\nu y$ on a part Γ of the boundary $\partial\Omega$, where ν denotes the outward unit normal vector on $\partial\Omega$.

It is well known that, for all complex data $(y^0, y^1) \in H_0^1(\Omega, \mathbb{C}) \times L^2(\Omega, \mathbb{C})$, there exists a unique solution $y \in C^0([0,T], H_0^1(\Omega, \mathbb{C})) \cap C^1((0,T), L^2(\Omega, \mathbb{C}))$ of (1) such that $y(0,x) = y^0(x)$ and $\partial_t y(0,x) = y^1(x)$ for every $x \in \Omega$.

Let y be the weak solution of (1)-(2). Supposing that the trace of $\partial_\nu y$ is measured on a measurable subset Γ of $\partial\Omega$ for all $t \in (0,T)$, find the initial data (y^0, y^1) in Ω.

The above problem belongs to a large family of inverse problems. It is known to be well posed whenever a so-called *observability property* is satisfied (see e.g. [22]).

In section 2, we explain how to model and solve the problem of optimizing the position and shape of the sensors for the physical model we have mentioned, based on an inequality called observability. Section 3 is dedicated to the study of sensor positioning for *thermo-acoustic tomography*. The notion of observability is not relevant in this context and the approach developed in Section 2 can no longer be used. This section shows the limitations of the approach presented in Section 2. We provide tracks to model and solve numerically the question of the optimal design of sensors in this framework.

§2. Optimal observability issues

Optimal locations of sensors issues have been widely studied in engineering, especially in applications such as structural acoustics, piezoelectric actuators or vibration control in mechanical structures. We mention in particular [1] for boundary actuators, [7] in the context of electrical impedance tomography. Numerical tools have been developed in [2, 8, 13, 21] to solve a simplified version of the optimal design problem where either the partial differential equation has been replaced with a discrete approximation, or the class of optimal designs is replaced with a compact finite-dimensional set.

The problem of optimizing the shape of the sensors, without any restriction on their complexity or regularity, is infinite-dimensional and has been only little considered. Let us nevertheless mention [9, 10] where the issue of determining the optimal damping term via its support for the 1D wave equation has been considered. They highlighted the well known *spillover phenomenon* arising when considering spectral approximations.

2.1. Modelling of the optimal design problem

The role of the sensors is to achieve some measurements over a time horizon $[0,T]$, with which one aims at reconstructing the whole state of the system over $[0,T]$. Let Γ be a measurable subset of $\partial\Omega$ standing for the domain occupied by sensors. Before modelling the optimal design problem, we need to recall that the inverse problem of recovering any initial data of (1)-(2) from the observation of the Neumann trace of y on Γ during a time T is known to be equivalent to the following observability property: there exists $C > 0$ such that for any solution y of (1), one has

$$C\|(y(0,\cdot), \partial_t y(0,\cdot))\|^2_{H_0^1(\Omega,\mathbb{C})\times L^2(\Omega,\mathbb{C})} \leq \int_0^T \int_{\partial\Omega} \chi_\Gamma(x) \left|\frac{\partial y}{\partial \nu}(t,x)\right|^2 d\mathcal{H}^{n-1}\, dt. \tag{3}$$

The best constant in this inequality is denoted $C_T(\Gamma)$. If $C_T(\Gamma) > 0$ then the system (1)-(2) is said to be *observable* in time T. Within the class of C^∞ domains, observability holds true if (Γ, T) satisfies the *Geometric Control Condition (GCC)* (see [3]), and this sufficient condition is almost necessary. We refer to [20, 22] for an overview of boundary observability results for wave-like equations.

Since the constant $C_T(\Gamma)$ can be interpreted as a measure of the well-posed character of the aforementioned inverse problem, it might a priori appear natural to model the problem of optimal observability as the one of maximizing the shape functional $\Gamma \mapsto C_T(\Gamma)$ over a well-chosen set of constraints. Nevertheless, for many reasons that have been much discussed in [16, 17, 18], the functional $C_T(\Gamma)$ does not appear as a so relevant criterion whenever one is allowed to perform a lot of measurements. Moreover, it is also highlighted in these references that using such an optimization criterion poses significant mathematical difficulties. Indeed, roughly speaking, this constant is *deterministic* and provides an account for the *worst possible case*. From a practical point of view, when a large number of measures is realized, one can expect that worst cases do not arise often, and therefore look for optimal observation domains in average. This drives us to rather consider what is referred to in the aforementioned works as *the randomized observability constant*. Inspired by the randomisation procedure introduced in [5, 6], this constant is associated with an average observability inequality. Let us briefly describe how to compute it. There is also another interpretation of this constant in terms of the long time asymptotics of the observability constant. One can refer for example to [11, 12] for more explanations on this approach.

Let $(\phi_j)_{j\in\mathbb{N}^*}$ be a Hilbert basis of $L^2(\Omega)$ consisting of eigenfunctions of the Dirichlet-Laplacian operator on Ω, associated with the negative eigenvalues $(-\lambda_j^2)_{j\in\mathbb{N}^*}$. Then any solution y of (1)-(2) can be expanded as

$$y(t,x) = \sum_{j=1}^{+\infty} \left(\frac{a_j}{\sqrt{\lambda_j}} e^{i\lambda_j t} + \frac{b_j}{\sqrt{\lambda_j}} e^{-i\lambda_j t} \right) \phi_j(x), \tag{4}$$

where the coefficients a_j and b_j belong to $\ell^2(\mathbb{C})$ and account for initial data.

By plugging this expression in (3), one shows that $C_T(\Gamma)$ reads as the infimum of

$$\int_0^T \int_\Gamma \left| \sum_{j=1}^{+\infty} \left(\frac{a_j}{\sqrt{\lambda_j}} e^{i\sqrt{\lambda_j} t} + \frac{b_j}{\sqrt{\lambda_j}} e^{-i\sqrt{\lambda_j} t} \right) \frac{\partial \phi_j}{\partial \nu} \right|^2 d\mathcal{H}^{n-1} dt$$

over the set of all sequences (a_j) and (b_j) in $\ell^2(\mathbb{C})$ such that $\sum_{j=1}^{+\infty} (|a_j|^2 + |b_j|^2) = 1$.

Selecting randomly all possible initial data for (1)-(2) leads to replace $C_T(\Gamma)$ with the so-called *random observability constant* denoted $C_{T,\mathrm{rand}}(\Gamma)$ and defined as the infimum of

$$\mathbb{E} \int_0^T \int_\Gamma \left| \sum_{j=1}^{+\infty} \left(\frac{\beta_{1,j}^\omega a_j}{\sqrt{\lambda_j}} e^{i\lambda_j t} + \frac{\beta_{2,j}^\omega b_j}{\sqrt{\lambda_j}} e^{-i\lambda_j t} \right) \frac{\partial \phi_j}{\partial \nu} \right|^2 d\mathcal{H}^{n-1}\, dt, \tag{5}$$

over the set of all sequences (a_j) and (b_j) in $\ell^2(\mathbb{C})$ such that $\sum_{j=1}^{+\infty} (|a_j|^2 + |b_j|^2) = 1$, where $(\beta_{1,j}^\omega)_{j\in\mathbb{N}^*}$ and $(\beta_{2,j}^\omega)_{j\in\mathbb{N}^*}$ are two sequences of independent random variables on a probability space $(A, \mathcal{A}, \mathbb{P})$ having mean equal to zero, variance equal to 1 and a super-exponential decay

(for instance, independent Bernoulli random variables, see [5, 6] for more details). Here, $\mathbb{E}$ is the expectation in the probability space, and runs over all possible events ω.

In spite of its intrinsic interest for the modeling of optimal shape design of sensors, the expression of the *random observability constant* can be significantly simplified, by using standard computations on random variables, as highlighted in the next result.

Proposition 1 ([18]). *Let $\Gamma \subset \partial\Omega$ be measurable. We have*

$$C_{T,rand}(\Gamma) = T \inf_{j\in\mathbb{N}^*} \frac{1}{\lambda_j} \int_\Gamma \left(\frac{\partial \phi_j}{\partial \nu}(x)\right)^2 d\mathcal{H}^{n-1}. \tag{6}$$

Although not so easy to handle, this expression of $C_{T,\mathrm{rand}}(\Gamma)$ can be numerically approximated by using an appropriate truncation (see Section 2.3).

We end this section by deriving a possible model for the optimal shape design of sensors problems.

Note first that, if one aims at maximizing $C_{T,\mathrm{rand}}(\Gamma)$ over every subset Γ of the boundary, it can be easily proved that the best solution is to take $\Gamma = \partial\Omega$ which is not relevant from a physical point of view. For this reason, we will consider some restriction on the set (of sensors) Γ, by imposing $\mathcal{H}^{n-1}(\Gamma) = L\mathcal{H}^{n-1}(\partial\Omega)$ for some $L \in [0,1]$. This constraint models the sensor usage cost.

Hence, let $L \in [0,1]$ and let us introduce the set

$$\mathcal{V}_L = \left\{\chi_\Gamma \,|\, \Gamma \subset \partial\Omega \text{ and } \mathcal{H}^{n-1}(\Gamma) = L\mathcal{H}^{n-1}(\partial\Omega)\right\}. \tag{7}$$

The problem of determining the optimal shape and location of boundary sensors we will consider reads

$$\boxed{\sup\{C_{T,\mathrm{rand}}(\Gamma),\ \chi_\Gamma \in \mathcal{V}_L\}}. \tag{8}$$

Remark 1. In [14, 15, 16, 17], where *internal* subsets were considered to be optimized, a closely related optimal design problem has been modeled, consisting of maximizing the infimum over all modes of $\int_O \phi_j(x)^2\,dx$, where O denotes a subset of Ω of prescribed Lebesgue measure. The study required assumptions on the asymptotics of ϕ_j^2, and led to take into account *quantum ergodicity properties*, i.e., asymptotic properties of the probability measures $\phi_j(x)^2\,dx$.

2.2. Analysis of the optimal design problem (8)

In view of analyzing the optimal design problem (8), it is convenient to consider a relaxed version of this problem. For $a \in L^\infty(\partial\Omega)$, we introduce

$$J_\infty(a) = T \inf_{j\in\mathbb{N}^*} \frac{1}{\lambda_j} \int_{\partial\Omega} a \left(\frac{\partial \phi_j}{\partial \nu}\right)^2 d\mathcal{H}^{n-1}$$

and the relaxed optimal design problem

$$\sup_{a\in\overline{\mathcal{V}}_L} J_\infty(a) \tag{9}$$

where

$$\overline{\mathcal{V}}_L = \left\{ a \in L^\infty(\partial\Omega, [0,1]) \mid \int_{\partial\Omega} a \, d\mathcal{H}^{n-1} = L\mathcal{H}^{n-1}(\partial\Omega) \right\}.$$

As a first step, we establish links between the two problems (8) and (9), which will prove that it is reasonable to focus on the relaxed problem (9).

Before stating a completely general result, let us first assume for the sake of simplicity that $n = 2$ and investigate two particular examples: the square $\Omega_{\rm sq} := (-\pi/2, \pi/2)^2$ and the unit disk Ω_{disk} of $\mathbb{R}^2$ centered at the origin. In these cases, it is possible to provide a complete analysis of Problems (8) and (9), by considering as a Hilbert basis of eigenfunctions.

- In the case of $\Omega_{\rm sq}$:

$$\phi_{n,k}(x,y) = \frac{2}{\pi} \sin\left(n\left(x + \frac{\pi}{2}\right)\right) \sin\left(k\left(y + \frac{\pi}{2}\right)\right), \tag{10}$$

  associated to the eigenvalue $\lambda_{n,k} = n^2 + k^2$, for all $(n,k) \in (\mathbb{N}^*)^2$.

- In the case of $\Omega_{\rm disk}$:

$$\phi_{jkm}(r,\theta) = \begin{cases} R_{0k}(r)/\sqrt{2\pi} & \text{if } j = 0, \\ R_{jk}(r) Y_{jm}(\theta) & \text{if } j \geq 1, \end{cases} \tag{11}$$

  for $j \in \mathbb{N}$, $k \in \mathbb{N}^*$ and $m = 1, 2$, where (r, θ) are the usual polar coordinates. The functions $Y_{jm}(\theta)$ are defined by $Y_{j1}(\theta) = \frac{1}{\sqrt{\pi}} \cos(j\theta)$ and $Y_{j2}(\theta) = \frac{1}{\sqrt{\pi}} \sin(j\theta)$, and R_{jk} by

$$R_{jk}(r) = \sqrt{2} \, \frac{J_j(z_{jk} r)}{|J_j'(z_{jk})|}, \tag{12}$$

  where J_j is the Bessel function of the first kind of order j, and $z_{jk} > 0$ is the $k^{\rm th}$-zero of J_j. The eigenvalues of the Dirichlet-Laplacian are given by the double sequence of $-z_{jk}^2$ and are of multiplicity 1 if $j = 0$, and 2 if $j \geq 1$.

Theorem 2 ([18])**.** *If Ω denotes either $\Omega_{\rm sq}$ or Ω_{disk}, the optimal values for Problem* (8) *and its convexified version* (9) *are the same, and moreover there exists a finite set $\mathcal{L} \subset [0,1]$ such that the optimal design problem* (8) *has a solution if, and only if $L \in \mathcal{L}$.*

Remark 2. It is furthermore notable that if $\Omega = \Omega_{\rm sq}$, then

$$\max_{a \in \overline{\mathcal{V}}_L} J_\infty(a) = \sup_{\chi_\Gamma \in \mathcal{V}_L} J_\infty(\chi_\Gamma) = \frac{4L}{\pi}.$$

and if $\Omega = \Omega_{disk}$, then

$$\max_{a \in \overline{\mathcal{V}}_L} J_\infty(a) = \sup_{\chi_\Gamma \in \mathcal{V}_L} J_\infty(\chi_\Gamma) = \pi L.$$

The fact that there is no-gap between both optimal values for the initial optimal design problem and its relaxed version can be extended to more general bounded connected open sets Ω of $\mathbb{R}^n$, under appropriate spectral assumptions on the domain Ω (satisfied in particular by $\Omega_{\rm disk}$ in dimension 2) that we will not state here because of their complexity. We refer to [18].

Theorem 3 ([18])**.** *Let Ω be a bounded connected domain of $\mathbb{R}^n$ with a $C^{1,1}$ boundary. Under strong assumptions on Ω (related to quantum ergodicity issues), the optimal values of Problems* (8) *and* (9) *are the same.*

Since it appears that the two optimization problems (8) and (9) are closely related, we will now focus on solving the relaxed problem, which can be solved explicitly in some cases. With this in mind, we are introducing special functions, which are natural[1] candidates for solving the problem (9).

Definition 1 (Rellich admissible functions)**.** Let Ω be a convex bounded connected domain of $\mathbb{R}^n$ and x_0 belong to $\overline{\Omega}$. We will say that the function $\tilde{a}_{x_0}$ defined by

$$\tilde{a}_{x_0}(x) = \frac{L\mathcal{H}^{n-1}(\partial\Omega)}{n|\Omega|}\langle x - x_0, \nu(x)\rangle, \tag{14}$$

for a.e. $x \in \partial\Omega$, is a *Rellich admissible function* of Problem (9) whenever it belongs to the admissible set $\overline{\mathcal{V}_L}$.

Remark 3. It is notable that, thanks to the convexity assumption on Ω, the function $\tilde{a}_{x_0}$ is nonnegative as soon as x_0 belongs to $\overline{\Omega}$.

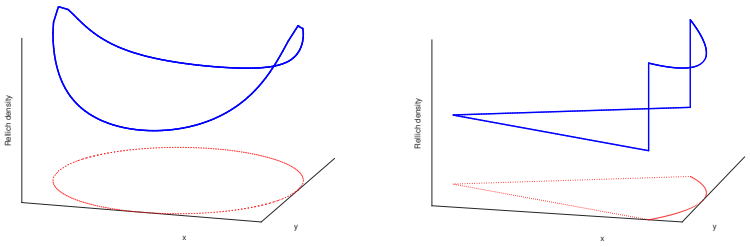

Figure 1: Plot of two Rellich densities (continuous line): for an ellipse (dotted line, left) and for an angular sector (dotted line, right).

We end this section by investigating the optimality of Rellich densities for Problem (9). To this aim, let us introduce the quantity $\ell_{\partial\Omega}(x_0)$ defined for $x_0 \in \mathbb{R}^n$ by

$$\ell_{\partial\Omega}(x_0) = \max_{x\in\partial\Omega} \|x - x_0\|.$$

It coincides with the distance from x_0 to the furthest point of $\partial\Omega$.

[1] The introduction of such functions rests upon the so-called Rellich identity, discovered by Rellich in 1940 (see [19]), which reads

$$\forall x_0 \in \mathbb{R}^n, \qquad 2 = \frac{1}{\lambda_j}\int_{\partial\Omega}\langle x - x_0, \nu(x)\rangle\left(\frac{\partial\phi}{\partial\nu}(x)\right)^2 d\mathcal{H}^{n-1}(x) \tag{13}$$

for every $C^{1,1}$ or convex bounded domain Ω of $\mathbb{R}^n$, where $\langle\cdot,\cdot\rangle$ is the Euclidean scalar product in $\mathbb{R}^n$, and for every eigenfunction ϕ of the Dirichlet-Laplacian operator.

Theorem 4. *Let $\Omega \subset \mathbb{R}^n$ be a convex bounded connected domain of $\mathbb{R}^n$. Introduce $L_n^c = \min\{1, L_n^*(\Omega)\}$ with*

$$L_n^*(\Omega) = \frac{n|\Omega|}{\mathcal{H}^{n-1}(\partial\Omega)\inf_{x_0\in\mathbb{R}^n} \ell_{\partial\Omega}(x_0)}. \tag{15}$$

Then, there exists a Rellich function $\tilde{a}_{x_0}$ (defined by (14)*) solving Problem* (9) *if and only if $L \in [0, L_n^c]$.*

2.3. Spectral truncations

Having in mind realistic applications, we claim that Theorems 2 and 3 provide an answer to the issue of optimizing the shape and location of sensors which is rather difficult to interpret.

As the measuring devices are not able to pick up too high frequencies, it seems reasonable to consider a modal approximation of the criterion J_∞, involving only a finite number of Laplacian eigenmodes. This leads us to introduce the functional J_N defined by

$$J_N(a) = \inf_{1\le j\le N} \frac{1}{\lambda_j} \int_{\partial\Omega} a \left(\frac{\partial\phi_j}{\partial\nu}\right)^2 d\mathcal{H}^{n-1}. \tag{16}$$

involving the N first modes of the Dirichlet-Laplace operator.

Let $M > 0$ and $L \in (0, 1)$. We will analyze the optimization problem

$$\sup_{a\in\overline{\mathcal{V}}_L} J_N(a) \tag{$\mathcal{P}_N$}$$

where $N \in \mathbb{N}^*$ is given.

Proposition 5. *Let $N \in \mathbb{N}^*$ and Ω denote either $\Omega_{\rm sq}$ or Ω_{disk}. Then, for every $L \in (0, 1)$, the optimal design problem ($\mathcal{P}_N$) has a (non unique) solution a_N which is bang-bang, in other words, which belongs to $\mathcal{V}_L$ defined by* (7)*.*

A more complete version of this result is provided in [18, Theorem 2]. It allows to deal with more general domains of $\mathbb{R}^n$, with $n \ge 2$, under an appropriate spectral property on the domain Ω.

We end this section by illustrating Proposition 5, representating solutions to Problem ($\mathcal{P}_N$) whenever Ω denotes a square or a elipse.

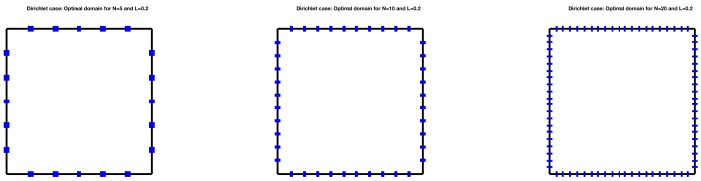

Figure 2: $\Omega = [-\pi/2, \pi/2]^2$ and $L = 0.2$. Examples of maximizers a_N^* for J_N and (from left to right) $N \in \{5, 10, 20\}$. The bold line corresponds to the set $\Gamma = \{a_N^* = 1\}$.

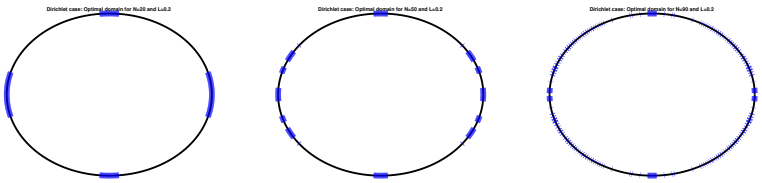

Figure 3: Ω is the ellipse having as cartesian equation $x^2 + y^2/2 = 1$ and $L = 0.2$. Examples of maximizers a_N^* for J_N and (from left to right) $N \in \{20, 50, 90\}$. The bold line corresponds to the set $\Gamma = \{a_N^* = 1\}$.

§3. Limitations of this approach: the *thermo-acoustic tomography* case

In this section, we take the opposite view of the approach presented so far. Indeed, we detail a particular application that we find interesting to show the limitations of the approach described in the previous section. It concerns *thermo-acoustic tomography*, a non-invasive medical imaging technique, for which it is indeed not possible to model the optimal design problem as we did previously. We will explain the reasons for this and propose a way to address this issue. This part is based on [4], a collaborative work with Élie Bretin and Maïtine Bergounioux.

Let us consider a simple model related to *thermo-acoustic tomography*. The principle is rather simple: the tissue to be visualized is irradiated by an electromagnetic radio-frequency pulse and this energy induces a heating process. This creates a thermally induced pressure surge that propagates as a sound wave, which can be detected by sensors located outside the body to image. By detecting pressure waves, heterogeneities can be observed: this gives important information such as the position and/or size of tumors in breast cancer.

If measurements are made to determine the initial pressure p_0, then the heterogeneities can be identified by quantitative estimates of electrical sensitivity and conductivity. We focus on the following question: *from the knowledge of a first series of measurements, how to locate the sensors before performing a second one, in a relevant way?*

Let Ω be a convex open subset of $\mathbb{R}^d$, representing the body to image, which means in particular that

$$\mathrm{supp}(p_0) \subset \Omega, \tag{17}$$

where $\mathrm{supp}(p_0)$ denotes the support of p_0. Let $\mathcal{B}$ be a ball with a large enough radius so that $\Omega \subset \mathcal{B}$; the set $\mathcal{B} \setminus \Omega$ stands for the ambient media (water or air), where the wave propagates.

The behaviour of the acoustic wave once the source p_0 is known, is described by

$$\begin{cases} \partial_{tt} p(t,x) - \mathrm{div}(c(x)\nabla p(t,x)) = 0 & \text{in } (0,T)\times\mathcal{B}, \\ p(0,\cdot) = p_0, & \text{in } \mathcal{B}, \\ \partial_t p(0,\cdot) = 0 & \text{in } \mathcal{B}, \\ p = 0 & \text{on } (0,T)\times\partial\mathcal{B}, \end{cases} \tag{18}$$

where $T > 0$ is arbitrary and $c \in L^\infty(\mathbb{R}^d)$ stands for the sound speed, satisfying

$$c(x) \geq c_0 > 0 \quad \text{a.e. } x \in \mathbb{R}^d.$$

A typical choice for c is to assume it piecewise constant, depending on the nature of the medium through which the wave travels, namely:

$$c = c_1 \mathbb{1}_{\Omega} + c_2 \mathbb{1}_{\mathcal{B}\setminus\Omega}, \quad \text{with } (c_1, c_2) \in (\mathbb{R}_+^*)^2. \tag{19}$$

In the framework introduced in Section 2, it is assumed that, in a certain sense, a reflection phenomenon of solutions at the boundary of the domain occurs. Such an assumption is not relevant for the application we are considering here since we basically look for the initial data and optimal sensor positions at the same time, which requires a dedicated method.

Notice that there exists $R > 0$ large enough such that, for every $p_0 \in H_0^1(\Omega)$, the solution of problem (18) coincides with the solution of

$$\begin{cases} \partial_{tt} p(t,x) - \operatorname{div}(c(x)\nabla p(t,x)) = 0 & \text{in } (0,T)\times\mathbb{R}^d, \\ p(0,\cdot) = p_0(\cdot) & \text{in } \mathbb{R}^d, \\ \partial_t p(0,\cdot) = 0 & \text{in } \mathbb{R}^d, \end{cases} \tag{20}$$

with the convention that the initial datum p_0 has been extended by 0 to the whole space $\mathbb{R}^d$. In what follows, according to the discussion above, we will choose R is large enough so that p vanishes on $\partial\mathcal{B}$ all along the recording process (i.e. for $t \le T$).

Sensors set. To model the sensors optimal positioning, we first describe the class of admissible designs/sensors to be considered. Introduce $\Sigma \subset \mathbb{R}^d$ as the subdomain of $\mathbb{R}^d$ occupied by sensors. Roughly speaking, we will assume that every connected component of Σ is located around the boundary of Ω and has a positive *thickness* ε. Precisely, we assume the existence of a measurable set $\Gamma \subset \partial\Omega$ such that

$$\Sigma = \{s + \mu\, \nu(s),\, s \in \Gamma, \mu \in [0,\varepsilon]\}, \tag{21}$$

where $\nu(s)$ denotes the outward unit normal to Ω at s (see Figure 4). The set Σ is thus supported by the annular ring

$$\widetilde{\partial\Omega} := \{s + \mu\nu(s),\, s \in \partial\Omega, \mu \in [0,\varepsilon]\}.$$

Let us introduce the class $\mathcal{U}_L$ of functions $a \in L^\infty(\widetilde{\partial\Omega})$ such that $a(s + \mu\nu(s)) = X(s)$ for a.e. $(s,\mu) \in \partial\Omega \times [0,\varepsilon]$ with $X \in \mathcal{V}_L$ (defined by (7)), in accordance with Fig. 4. It models admissible subsets $\Gamma \subset \widetilde{\partial\Omega}$.

Optimal location after a first series of measurements. Let $p_{obs} \in L^2((0,T)\times\Sigma)$ denote the measured pressure: it is defined in $(0,T)\times\Sigma$. We extend p_{obs} by 0 to $(0,T)\times\mathcal{B}$ and denote the obtained function similarly, with a slight abuse of notation. Hence, one has $p_{obs} = \mathbb{1}_\Sigma\, p_{obs}$ so that $p_{obs} \in L^2(0,T,L^2(\mathcal{B}))$. For $p_0 \in H_0^1(\Omega)$, we also introduce $p_{[p_0]}$ as the solution of Problem (18) for the initial datum p_0.

The issue we address hereafter is: *given a first (series of) measurement(s), how can we determine a relevant sensor position before performing a new (series of) measurement(s)?*

Our approach can be split into two steps that we roughly describe.

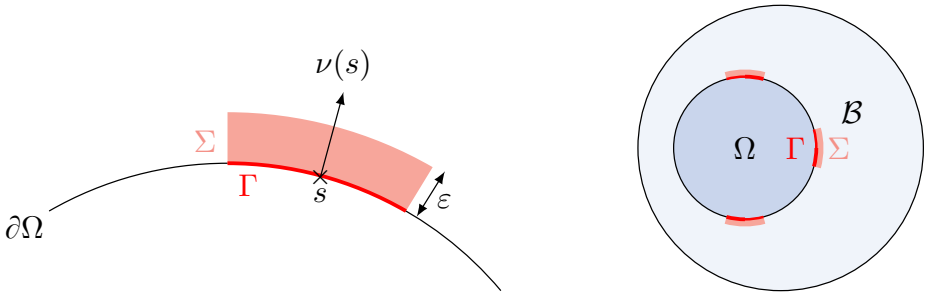

Figure 4: The set of sensors.

First step: determination of an initial pressure condition p_0. Recall that, in the PDE model we consider (see Eq. (18)), $\partial_t p(0,\cdot)$ is assumed to vanish identically in $\mathcal{B}$. It is therefore enough to reconstruct the initial pressure. A natural idea is to consider the problem

$$\inf_{p_0\in\mathcal{P}_0(\Omega)} A_1(\mathbb{1}_\Sigma, p_0) \tag{22}$$

where the expression of $A_1(\mathbb{1}_\Sigma, p_0)$ is

$$\frac{1}{2}\int_0^T\int_{\mathcal{B}} \mathbb{1}_\Sigma(x)(p_{[p_0]}(t,x) - p_{obs}(t,x))^2\,dx\,dt, \tag{23}$$

where $\mathcal{P}_0(\Omega)$ is the subspace of $H_0^1(\Omega)$ of positive functions whose support is included in a fixed compact set of $\mathcal{B}$.

Solving the resulting problem (see its definition below) is a way to define an initial pressure function $\widetilde{p_0}$ reconstructed (almost) everywhere in $\mathcal{B}$ and not only on Σ. This is the key point to address the optimal design problem in the second step.

Second step: determination of the best position of sensors. Once an initial pressure $\widetilde{p_0}$ has been determined with a given position of sensors, the new position will be obtained by solving the optimal design problem

$$\sup_{\mathbb{1}_\Sigma\in\mathcal{U}_L} A_2(\mathbb{1}_\Sigma, p_0),$$

where

$$A_2(\mathbb{1}_\Sigma, p_0) := \frac{\int_0^T\int_{\mathcal{B}} \mathbb{1}_\Sigma(x)\partial_t p_{[\widetilde{p_0}]}(t,x)^2\,dx\,dt}{\|p_0\|^2_{H^1(\Omega)}}. \tag{24}$$

The functional to maximize represents the quality of the observation and is inspired by the expression of $C_T(\Gamma)$ in Section 2.1. Roughly speaking, we are looking for the position

of the sensors allowing the best observation of the worst possible pressure p_0 leading to the observation p_{obs}.

Detailed explanations of this approach can be found in [4]. In particular, it is explained how to modify the modeling above to take into account a finite number of sensors. The simulations below provide promising results on a toy problem involving a finite number of sensors.

All the numerical simulations done with the following set of parameters:

- the set Ω is a two-dimensional ball of radius 1
- the box $\mathcal{B} = [-D/2, D/2]^d$ has size $D = 4$ and the recording time is $T = 2$;
- the set K is a two-dimensional ball of radius 0.85
- we use a regular time step discretization $dt = T/2^{10}$ and $dx = D/2^9$.
- the thickness parameter ε is equal to 0.03.

To avoid the so-called inverse crime, we also use two different grids to compute the solution of the direct and inverse problems:

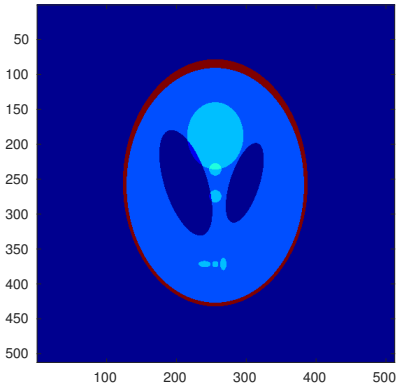

Figure 5: Initial source p_0.

§4. Conclusion

This article is a first attempt to

- model and solve the problem of optimizing the number, the position or the shape of sensors in order to improve the estimation of the state;
- efficiently locate sensors in the highly sensitive context of *thermo-acoustic tomography* where the standard framework of boundary observability does not hold anymore.

While the first theoretical and numerical results appear promising, we plan to investigate this issue further by examining other kinds of boundary conditions, 3D numerical experiments and how to discretize efficiently such kinds of optimal design problems to recover the properties of the continuous models.

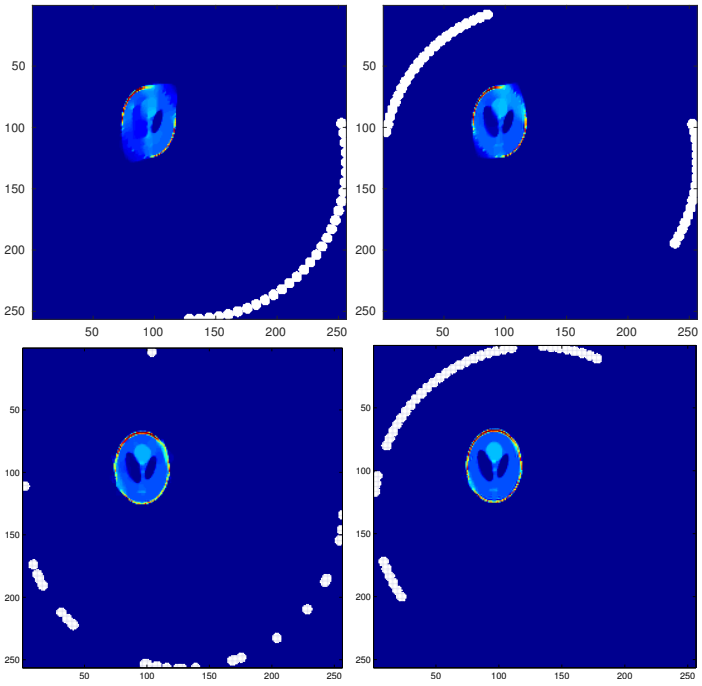

Figure 6: Optimization of sensors position. Each line corresponds to a different choice of the initial location of the sensors; Left: reconstructed source p_0^n after $n = 30$ iterations by using initial positions of the sensors; right: reconstructed source p_0^n after $n = 20$ iterations by using the new position of sensors.

Acknowledgements

The author was partially supported by the Project "Analysis and simulation of optimal shapes - application to lifesciences" of the Paris City Hall.

References

[1] Afifi, L., Chafiai, A., and El Jai, A. Spatial compensation of boundary disturbances by boundary actuators. *Applied Mathematics And Computer Science 11*, 4 (2001), 899–920.

[2] Armaou, A., and Demetriou, M. A. Optimal actuator/sensor placement for linear parabolic pdes using spatial h^2 norm. *Chemical Engineering Science 61*, 22 (2006), 7351–7367.

[3] Bardos, C., Lebeau, G., and Rauch, J. Sharp sufficient conditions for the observation, control, and stabilization of waves from the boundary. *SIAM journal on control and optimization 30*, 5 (1992), 1024–1065.

[4] Bergounioux, M., Bretin, E., and Privat, Y. How to position sensors in thermo-acoustic tomography. *Inverse Problems 35*, 7 (2019), 074003, 25. Available from: https://doi.org/10.1088/1361-6420/ab0e4d.

[5] Burq, N. Large-time dynamics for the one-dimensional schrödinger equation. *Proceedings of the Royal Society of Edinburgh: Section A Mathematics 141*, 02 (2011), 227–251.

[6] Burq, N., and Tzvetkov, N. Random data cauchy theory for supercritical wave equations i: local theory. *Inventiones mathematicae 173*, 3 (2008), 449–475.

[7] Dardé, J., Hakula, H., Hyvönen, N., Staboulis, S., and Somersalo, E. Fine-tuning electrode information in electrical impedance tomography. *Inverse Probl. Imaging 6* (2012), 399–421.

[8] Harris, T. J., Macgregor, J., and Wright, J. Optimal sensor location with an application to a packed bed tubular reactor. *AIChE Journal 26*, 6 (1980), 910–916.

[9] Hébrard, P., and Henrot, A. Optimal shape and position of the actuators for the stabilization of a string. *Systems & control letters 48*, 3 (2003), 199–209.

[10] Hébrard, P., and Henrot, A. A spillover phenomenon in the optimal location of actuators. *SIAM journal on control and optimization 44*, 1 (2005), 349–366.

[11] Humbert, E., Privat, Y., and Trélat, E. Observability properties of the homogeneous wave equation on a closed manifold. *Comm. Partial Differential Equations 44*, 9 (2019), 749–772. Available from: https://doi.org/10.1080/03605302.2019.1581799.

[12] Humbert, E., Privat, Y., and Trélat, E. Geometric and probabilistic results for the observability of the wave equation. *J. Éc. polytech. Math. 9* (2022), 431–461. Available from: https://doi.org/10.5802/jep.186.

[13] Morris, K. Linear-quadratic optimal actuator location. *Automatic Control, IEEE Transactions on 56*, 1 (2011), 113–124.

[14] Privat, Y., Trélat, E., and Zuazua, E. Optimal location of controllers for the one-dimensional wave equation. *Ann. Inst. H. Poincaré Anal. Non Linéaire 30*, 6 (2013), 1097–1126. Available from: http://dx.doi.org/10.1016/j.anihpc.2012.11.005.

[15] Privat, Y., Trélat, E., and Zuazua, E. Optimal observation of the one-dimensional wave equation. *J. Fourier Anal. Appl. 19*, 3 (2013), 514–544. Available from: http://dx.doi.org/10.1007/s00041-013-9267-4.

[16] Privat, Y., Trélat, E., and Zuazua, E. Optimal shape and location of sensors for parabolic equations with random initial data. *Arch. Ration. Mech. Anal. 216*, 3 (2015), 921–981. Available from: http://dx.doi.org/10.1007/s00205-014-0823-0.

[17] Privat, Y., Trélat, E., and Zuazua, E. Optimal observability of the multi-dimensional wave and Schrödinger equations in quantum ergodic domains. *J. Eur. Math. Soc. (JEMS) 18*, 5 (2016), 1043–1111. Available from: http://dx.doi.org/10.4171/JEMS/608.

[18] Privat, Y., Trélat, E., and Zuazua, E. Spectral shape optimization for the Neumann traces of the Dirichlet-Laplacian eigenfunctions. *Calc. Var. Partial Differential*

Equations 58, 2 (2019), Art. 64, 45. Available from: https://doi.org/10.1007/s00526-019-1522-3.

[19] Rellich, F. Darstellung der eigenwerte von $\delta u + \lambda u = 0$ durch ein randintegral. *Mathematische Zeitschrift 46*, 1 (1940), 635–636.

[20] Tucsnak, M., and Weiss, G. *Observation and control for operator semigroups*. Springer Science & Business Media, 2009.

[21] Wouwer, A. V., Point, N., Porteman, S., and Remy, M. An approach to the selection of optimal sensor locations in distributed parameter systems. *Journal of process control 10*, 4 (2000), 291–300.

[22] Zuazua, E. Controllability and observability of partial differential equations: some results and open problems. *Handbook of differential equations: evolutionary equations 3* (2007), 527–621.

Yannick Privat
Université de Strasbourg, CNRS UMR 7501, INRIA
Institut de Recherche Mathématique Avancée (IRMA) & Institut Universitaire de France (IUF)
7 rue René Descartes, 67084 Strasbourg, France
yannick.privat@unistra.fr